5,5′-Bridged Bis(1,2,3-dithiazoles): Spin States and Charge-Transfer Chemistry

Tosha M. Barclay,[1a] Leanne Beer,[1b] A. Wallace Cordes,[1a] Richard T. Oakley,*[,1b] Kathryn E. Preuss,[1b] Robert W. Reed,[1b] and Nicholas J. Taylor[1b]

Department of Chemistry and Biochemistry, University of Arkansas, Fayetteville, Arkansas 72701, and Department of Chemistry, University of Waterloo, Waterloo, Ontario N2L 3G1, Canada

Received September 6, 2000

Bifunctional 1,2,3-dithiazoles bridged with azine and phenylenediamine spacers have been prepared, with a view to determining the extent of communication between the two dithiazole rings as a function of the electronic and steric demands of the bridge. The crystal structure of the closed-shell diazine derivative [S_2NClC_2═NN═C_2ClNS_2] is rigorously planar. Cyclic voltammetry on this compound indicates two reversible one-electron oxidations. The radical cation state has been characterized by EPR spectroscopy and by crystal structure determination of its 1:1 PF_6^- salt. The latter reveals little interaction between neighboring radical cations; consistently, the material exhibits a conductivity of $\sigma < 10^{-5}$ S cm^{-1}. Insertion of a phenylene group into the diazine bridge to afford [S_2NClC_2═NC_6H_4N═C_2ClNS_2] leads to significant torsional motion between the phenylene ring and the two end groups, as a result of which the two DTA rings are electronically independent; no radical cation state has been observed for this species. Crystal data for $Cl_2S_4N_4C_4$: $a = 5.1469(15)$, $b = 13.343(2)$, $c = 14.2031(17)$, orthorhombic, *Pbca*, $Z = 4$. Crystal data for $Cl_2S_4N_4C_4PF_6$: $a = 11.699(4)$, $b = 12.753(5)$, $c = 10.461(4)$, $\beta = 112.17(1)°$, monoclinic, *C*2/*c*, $Z = 4$. Crystal data for $C_{l2}S_4N_4C_{10}H_4$: $a = 3.9477(6)$, $b = 23.790(3)$, $c = 7.3769(9)$, $\beta = 90.793(12)°$, monoclinic, $P2_1/c$, $Z = 2$.

Introduction

The chemistry of 1,2,3-dithiazole (DTA) compounds has been studied extensively.[2] Historically, the pursuit of these materials has been driven by their applications in agriculture, e.g., as herbicides and fungicides. More recently, the potential utility of DTA derivatives in materials science has emerged.[3] DTA radicals (**1**)[4] have been used as building blocks for neutral radical conductors,[5] and benzo- and naphtho-fused bis(dithiazoles) have been shown to have a rich charge-transfer (CT) chemistry.[6,7] Although they are not particularly strong donors, these compounds, along with the recently reported 5,5′-bridged fulvalene compound (**2**),[8] can be oxidized to stable, highly delocalized radical cations that serve as templates for the formation of conductive CT salts.[9,10]

As part of continuing work on 5,5′-bridged bis(DTAs)**,** we report the preparation of derivatives possessing azine (**3**) and phenylenediamine (**4**) spacers between the two DTA rings; like **2**, compounds **3** and **4** are closed-shell rather than diradical species. The structures and redox chemistry of both compounds have been explored using a combination of crystallography, cyclic voltammetry, and EPR spectroscopy. Density functional theory (DFT) calculations on **3** have been performed to probe the energy difference between the closed-shell singlet and diradical triplet states and also to establish the electronic structure of and spin distribution within the radical cation [**3**]$^+$. A crystalline derivative of [**3**]$^+$ has been isolated and characterized by EPR spectroscopy and X-ray crystallography.

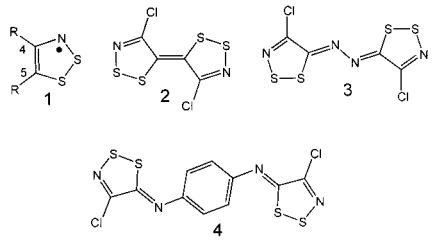

Results and Discussion

Synthesis. The starting material for the preparation of both **3** and **4** is 4,5-dichlorodithiazolylium chloride (**5**), commonly known as Appel's salt.[11] The substitution chemistry of **5** with nucleophiles, notably amines, has been widely studied.[2] Its reactivity with azines has also been explored,[12] but no bifunctional derivative, with two bridged DTA rings, has ever been isolated. In this work, we have found that the reaction of 1,4-

(1) (a) University of Arkansas. (b) University of Waterloo.
(2) Kim, K. *Sulfur Rep.* **1998**, *21*, 147.
(3) (a) Rawson, J. M.; McManus, G. D. *Coord. Chem. Rev.*, **1999**, *189*, 135. (b) Torroba, T. *J. Prakt. Chem.* (*Weinheim, Ger.*) **1999**, *341*, 99.
(4) Barclay, T. M.; Beer, L.; Cordes, A. W.; Oakley, R. T.; Preuss, K. E.; Taylor, N. J.; Reed, R. W. *Chem. Commun.* **1999**, 531.
(5) Barclay, T. M.; Cordes, A. W.; Haddon, R. C.; Itkis, M. E.; Oakley, R. T.; Reed, R. W.; Zhang, H. Z. *J. Am. Chem. Soc.* **1999**, *121*, 969.
(6) Barclay, T. M.; Cordes, A. W.; Goddard, J. D.; Mawhinney, R. C.; Oakley, R. T.; Preuss, K. E.; Reed, R. W. *J. Am. Chem. Soc.* **1997**, *119*, 12136.
(7) Barclay, T. M.; Cordes, A. W.; Oakley, R. T.; Preuss, K. E.; Reed, R. W. *Chem. Mater.* **1999**, *11*, 164.
(8) Barclay, T. M.; Cordes, A. W.; Oakley, R. T.; Preuss, K. E.; Reed, R. W. *Chem. Commun.* **1998**, 1039.
(9) Barclay, T. M.; Beer, L.; Cordes, A. W.; Haddon, R. C.; Itkis, M. E.; Oakley, R. T.; Preuss, K. E.; Reed, R. W. *J. Am. Chem. Soc.* **1999**, *121*, 6657.
(10) Barclay, T. M.; Burgess, I. J.; Cordes, A. W.; Oakley, R. T.; Reed, R. W. *Chem. Commun.* **1998**, 1939.
(11) (a) Appel, R.; Janssen, H.; Siray, M.; Knoch, F. *Chem. Ber.* **1985**, *118*, 1632. (b) Besson, T.; Dozias, M.-J.; Guillard, J.; Rees, C. W. *J. Chem. Soc., Perkin Trans. 1* **1998**, 3925.
(12) (a) Cuadro, A. M.; Alvarez-Builla, J. *Tetrahedron* **1994**, *50*, 10037. (b) L'abbé, G.; D'hooge, B.; Dehaen, W. *J. Chem. Soc., Perkin Trans. 1* **1995**, 2379.

10.1021/ic0010095 CCC: $20.00
Published on Web 04/21/2001

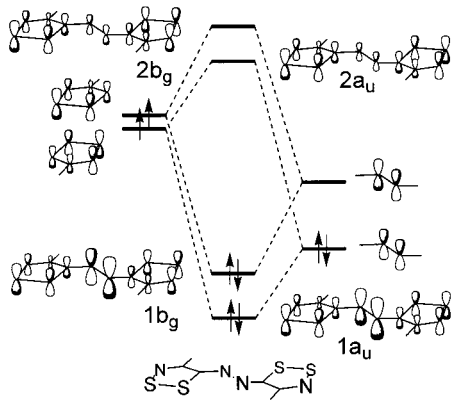

Figure 1. Frontier molecular orbitals arising from the interactions of two 1,2,3-DTA radicals with a bridging N_2 unit.

phenylenediamine with an excess of Appel's salt yields what we presume is the doubly oxidized dichloride salt [**4**][Cl]$_2$ (eq 1). This insoluble solid is easily reduced with ethanol to the

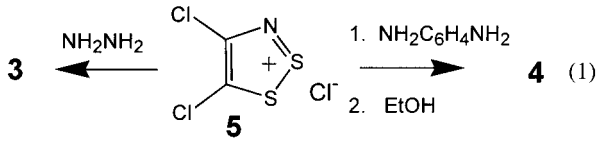

(1)

neutral **4**, which can be recrystallized from toluene as red, air-stable needles. The compound is diamagnetic (EPR silent), and the molecular structural features (vide infra) are consistent with a closed-shell formulation. The preparation of **3** follows from that used for **4**, although in this case, no intermediate oxidized state has been observed; the reaction of Appel's salt (eq 1) with exactly 2 equiv of anhydrous hydrazine proceeds directly to **3**. The product can be recrystallized from chlorobenzene or toluene as red flakes with a green opalescence. Blocklike crystals suitable for X-ray work can be grown by sublimation in vacuo. This compound is also diamagnetic, and like **2** and **4**, its electronic structure is best represented by the closed-shell formulation **3**.

Electronic Structure of 3. The potential use of the azine group as a building block for conductive polymers has attracted some interest,[13] and it is known that end-group effects can have a profound impact on the electronic and molecular structure of the azine chromophore.[14] In this work, we have been equally interested in the influence of the azine group on the redox behavior of the two DTA rings. The possible electronic states arising from the coupling of two DTA rings (**1**) directly at carbon has been explored by several groups.[9,15] Linkage via the 4,4′-positions is predicted to induce a diradical structure **6** (akin to the disjoint bis-dithiadiazolyl **7**),[16] while fusion at the 5,5′-carbons is known to a closed-shell fulvalene structure, as in **2**.[9] Incorporation of a bridging azine group likewise produces a closed-shell species, but the effect of the bridge on the spin state and redox properties of the consequent azine-bridged compound is not immediately clear. Figure 1 illustrates the frontier molecular orbital (FMO) interactions arising when two DTA radicals are linked at the 5,5′-positions by a dinitrogen bridge. Of particular importance is the effect of the high electronegativity of the N_2 bridge on the electronic distribution; it stabilizes the singlet state relative to the diradical triplet by lowering the highest occupied molecular orbital (HOMO) (relative to that in **2**) and polarizes the two occupied π-levels onto the azine bridge. As a result, the CT chemistry of **3** will involve the removal of electrons localized more on the bridge than on the two DTA end groups.

Table 1. Summary of Bond Lengths (Å) and Mulliken Atomic Charges (q) for **1** and [**1**]$^+$ ($R_{4,5}$ = H)[a]

	bond lengths			charges	
state	**1** (^{2}A″)	[**1**]$^+$ (^{1}A′)		**1** (^{2}A″)	[**1**]$^+$ (^{1}A′)
S−S	2.154	2.099	$q_{S(C)}$	0.099	0.397
S−N	1.665	1.602	$q_{S(N)}$	0.274	0.564
S−C	1.744	1.681	q_N	−0.470	−0.348
N−C	1.334	1.324	$q_{C(N)}$	0.128	0.154
C−C	1.386	1.409	$q_{C(S)}$	−0.317	−0.267

[a] B3LYP/6-31G** optimized geometries in C_s symmetry.

Table 2. Energies,[a] Computed Bond Lengths (Å), and Mulliken Atomic Charges (q) for the Proto Variant of **3**

state	**3** (^{1}A$_g$)	**3** (^{3}B$_u$)	[**3**]$^+$ (^{2}B$_g$)	[**3**]$^{2+}$ (^{1}A$_g$)
energy	−1965.316 15	−1965.267 46	−1965.048 42	−1964.619 30
	(0.00)	(1.32)	(7.29)	(18.96)
S−S	2.1382	2.1254	2.1038	2.0853
S−N	1.6707	1.6681	1.6362	1.6009
S−C	1.7843	1.7774	1.7526	1.7271
N−C	1.2901	1.3242	1.3037	1.3228
C−C	1.4559	1.4012	1.4364	1.4168
C−N	1.2961	1.3636	1.3333	1.3880
N−N′	1.3678	1.287	1.3178	1.2668
$q_{S(C)}$	0.1097	0.1367	0.2718	0.4152
$q_{S(N)}$	0.2751	−0.4690	0.4693	0.6530
q_N	−0.4309	−0.4690	−0.3888	−0.3366
$q_{C(N)}$	0.1348	0.1328	0.1580	0.1829
$q_{C(S)}$	0.0770	0.0161	0.0493	0.0168
$q_{N(N)}$	−0.3229	−0.2710	−0.2648	−0.1831

[a] In Hartrees, from B3LYP/6-31G** optimized geometries in C_{2h} symmetry. Numbers in parentheses are relative energies in eV.

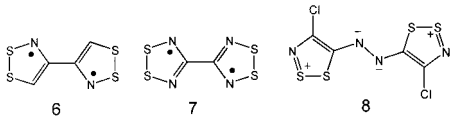

To quantify these FMO ideas, we have carried out density functional theory (B3LYP/6-31G**) calculations on a series of model compounds, i.e., proto variants of **1**, **2**, and **3**. Table 1 indicates the changes in structure and charge distribution that accompany oxidation of a 1,2,3-DTA radical (**1**) ($R_{4,5}$ = H), and Table 2 provides a similar analysis for a diazine-bridged compound, bis(DTA).[17] The numerical details support the qualitative conclusions outlined above. First, the diradical (triplet) state of the azine-bridged compound is more high-lying (1.32 eV) relative to the singlet than is that of the directly fused fulvalene (**2**) (0.94 eV) relative to its singlet.[9] Second, from the charge distribution, it is apparent that a diazine-bridged bis-(DTA) is best described using a covalent formulation (as in **3**) rather than by means of a mesoionic structure such as **8**. First and second oxidation strips electrons from the 1b$_g$ HOMO,

(13) Bethell, D.; Kang, D.-H.; Zerbi, G. *J. Chem. Soc., Perkin Trans. 2* **1996**, 1081.
(14) Euler, W. B.; Cheng, M.; Zhao, C. *Chem. Mater.* **1999**, *11*, 3702.
(15) Genin H.; Hoffmann, R. *Macromolecules* **1998**, *31*, 444.
(16) Bryan, C. D.; Cordes, A. W.; Goddard, J. D.; Haddon, R. C.; Hicks, R. G.; MacKinnon, C. D.; Mawhinney, R. C.; Oakley, R. T.; Palstra, T. T. M.; Perel, A. S. *J. Am. Chem. Soc.* **1996**, *118*, 330.
(17) The results shown refer to calculations performed on the molecular configuration found in the crystal structure of **3** (R = Cl). An alternative C_{2h} geometry for **3** (R = H), with the two DTA rings rotated by 180° about the exocyclic C−N bond, was also explored at the B3LYP/6-31G** level. The results afforded qualitatively similar conclusions with respect to charge distributions and bond lengths, but the ground-state singlet was 5.2 kcal mol^{-1} higher in energy.

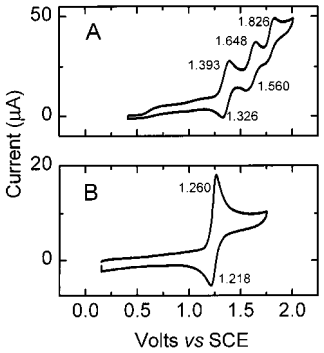

Figure 2. Cyclic voltammograms (sweep rate 100 mV) showing peak potentials of compounds **3** (A) and **4** (B) in CH_3CN, containing 0.1 M *n*-Bu_4NPF_6. Corresponding peak-to-peak separations for internal references: (A) ferrocene, 62 mV; (B) ferrocene, 67 mV.

Table 3. Solution Redox Potentials[a] for 1,2,3-Dithiazolyls

compound	**1**[b]	**2**	**3**	**4**
$E_{1/2}^{(0/+)}$	0.38	0.80	1.36	1.24
$E_{1/2}^{(+/2+)}$		1.25	1.60	
$E_{1/2}^{(2+/3+)}$			1.83[c]	
$E_{pc}^{(0/-)}$	−1.1[d]	−1.11[d]	−0.91[d]	−1.13[d]

[a] Volts vs SCE, in CH_3CN, 0.1 M *n*-Bu_4NPF_6. [b] Compound **1** with $R_5 = C_6F_5$, $R_4 = Cl$. [c] Irreversible oxidation, E_{pa} reported. [d] Irreversible reduction, E_{pc} reported.

which is strongly antibonding over the N−N region. The dication then becomes a diazo-bridged bis(thiazolylium) species, with internal S−S, S−N, and N−C bond lengths resembling those found in a simple $[DTA]^+$ cation.

Cyclic Voltammetry. We have explored the manifold of oxidation states potentially available to **3** and **4** by means of cyclic voltammetry. Representative voltammograms for the oxidation processes are illustrated in Figure 2 , and numerical results are compiled in Table 3, along with those found previously for **2** and **1** ($R_4 = Cl$, $R_5 = C_6F_5$). In both systems studied, the peak-to-peak separation of the ferrocene (Fc) internal reference was within the range of 62−67 mV (regardless of scan rate).

Typically, for a simple 1,2,3-DTA radical, a reversible oxidation to the closed-shell cation is observed near 0.3 V vs SCE, along with an irreversible reduction to the closed-shell anion near −1 V.[18] Both **3** and **4** show this strongly irreversible reduction process near −1 V, but their oxidation chemistry is more complex. Bridging two 1,2,3-DTA radicals at the 5-positions by electron-withdrawing azine or phenylenediamine spacers results in a closed-shell structure that is more resistant to oxidation. Consistently, oxidation of **3** and **4** requires more anodic potentials than, for example, those found for the fulvalene compound **2** or the 1,2,3-DTA radical **1** ($R_4 = Cl$, $R_5 = C_6F_5$). The potentials are also considerably more anodic than those seen in mesoionic diazine compounds such **9** and **10**.[19] In the case of **3**, stepwise reversible oxidation affords a radical cation $[\mathbf{3}]^+$ and a closed-shell dication $[\mathbf{3}]^{2+}$. The separation between these two waves (0.24 V) is, however, much less than in **2** (0.45 V). Interestingly, a third irreversible oxidation peak is also observed, and this we assign to oxidation of the diazo bridge in $[\mathbf{3}]^{2+}$. In compound **4**, the azine group is now itself bridged by a phenylene ring, and only a single oxidation wave with peak-to-peak separation of 42 mV (cf. 67 mV for Fc/Fc^+) is observed. This behavior is broadly consistent with the presence of two noninteracting one-electron processes, leading to the formation of $[\mathbf{4}]^{2+}$.[20]

The CV results on **3** and **4** can be compared to the findings of electrochemical studies on other azine-bridged compounds.[13,21] A recent report[19] on the redox manifold of mesoionic **9** and **10** revealed a manifold of four reversible waves (two oxidation, two reduction) for **9**. Incorporation of a phenylene ring, as in **10**, leads to a coalescence of the two reduction waves, as observed here (for **4**).

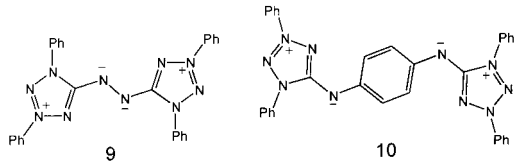

Radical Cation $[3]^+$. The stepwise oxidation of **3** observed in the CV experiments described above encouraged us to pursue the characterization of the radical cation $[\mathbf{3}]^+$. However, chemical oxidation of **3** to its radical cation state proved to be a difficult task. The high first oxidation potential $E_{1/2}^{(0/+)}$, coupled with the proximity of the second wave $E_{1/2}^{(+/2+)}$, made it difficult to access the desired state directly. For example, bromine and sulfuryl chloride failed to react with **3** at all, while chlorine and nitrosonium salts carried the oxidation too far. Our initial approach to the problem consisted of reacting 2 mol equiv of $NOSbF_6$ with **3** to generate the putative dication salt $[\mathbf{3}][SbF_6]_2$ as a dark red solid. Comproportionation of this solid with neutral **3** in liquid SO_2 afforded turquoise solutions that displayed a strong EPR signal (vide infra) corresponding to the radical cation $[\mathbf{3}]^+$. Eventually, we were able to reach the radical cation specifically by using iodine trichloride in SO_2(l) as oxidant. On the basis of mass recovery and the need to use one-third of an equivalent of ICl_3 per mole of **3**, the crude black solid product so obtained was, we believed, $[\mathbf{3}][ICl_2]$. Accordingly, treatment of this crude solid with gallium trichloride in SO_2(l) afforded a golden, microcrystalline tetrachlorogallate salt, but attempts to recrystallize this material were unsuccessful. However, metathesis of $[\mathbf{3}][ICl_2]$ with $AgPF_6$ in SO_2(l) afforded a hexafluorophosphate salt $[\mathbf{3}][PF_6]$ in two morphologies, gold needles and black trapezoidal blocks. Both forms were extremely moisture sensitive, but X-ray analysis of the latter was nonetheless accomplished (vide infra). Pressed pellet measurements on this material indicated a low electronic conductivity, $\sigma < 10^{-5}$ S cm^{-1}.

When dissolved in SO_2(l), turquoise solutions of $[\mathbf{3}][PF_6]$ give rise to a strong EPR signal (Figure 3), the 1:2:3:2:1 fine structure of which heralds hyperfine coupling to two equivalent ^{14}N nuclei ($I = 1$) with $a_N = 0.236$ mT. Initial inspection of the appearance of this spectrum led us to speculate as to whether the fine structure arose from coupling to the two internal (azine) nitrogens or to the two DTA nitrogens. The former assignment was confirmed by cross-matching the experimental a_N values with those predicted by B3LYP/6-31G** calculations (Table 4). Consistent with the simple FMO ideas portrayed in Figure 1, removal of an electron from the $1b_g$ HOMO leads to a spin

(18) In condensed ring 1,2,3-DTA radicals, the reduction wave becomes reversible. See ref 5.

(19) Araki, S.; Yamamoto, K.; Inoue, T.; Fujimoto, K.; Yamamura, H.; Kawai, M.; Butsugan, Y.; Zhou, J.; Eichhorn, E.; Rieker, A.; Huber, M. *J. Chem. Soc., Perkin Trans. 2* **1999**, 985.

(20) (a) Bard, A. J.; Faulkner, L. R. *Electrochemical Methods, Fundamentals and Applications*; Wiley: New York, 1980. (b) Polcyn, D. S.; Shain, I. *Anal. Chem.* **1966**, *38*, 370.

(21) Osborne, A. G.; Webba da Silva, M.; Hursthouse, M. B.; Malik, K. M. A.; Opromolla, G.; Zanello, P. *J. Organomet. Chem.* **1996**, *516*, 167.

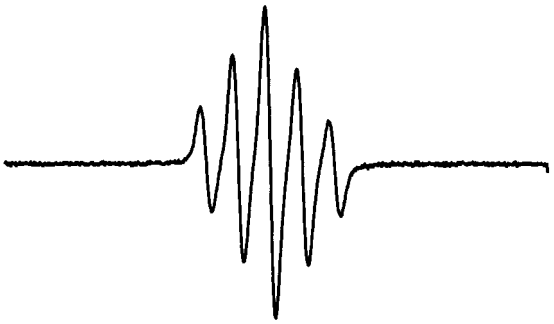

Figure 3. X-band EPR spectrum of $[\mathbf{3}]^+$ radical cation in SO_2(l), g = 2.0102, a_N = 0.236 mT (2 N). Sweep width 4.0 mT.

Table 4. g-Values, ^{14}N Isotropic Hyperfine Coupling Constants a_N (in mT), and Computed[a] Spin Densities

compound	**1**	$[\mathbf{2}]^+$	$[\mathbf{3}]^+$
g	2.0089[b]	2.0177	2.0102
a_N (observed)	0.61[b]	0.096	(DTA), 0.236 (azine)
ρ_N (calculated)	0.385[c]	0.056	0.018 (DTA), 0.55 (azine)
a_N (calculated)	0.695[c]	0.109	0.041 (DTA), 0.256 (azine)

[a] B3LYP/6-31G** values refer to the proto variants. [b] $R_5 = C_6F_5$, R_4 = Cl. [c] $R_5 = R_4$ = H.

Table 5. Crystallographic Data for **3**, [**3**][PF_6], and **4**

	3	[**3**][PF_6]	**4**
formula	$Cl_2S_4N_4C_4$	$Cl_2S_4N_4C_4PF_6$	$C_{l2}S_4N_4C_{10}H_4$
a, Å	5.1469(15)	11.699(4)	3.9477(6)
b, Å	13.343(2)	12.753(5)	23.790(3)
c, Å	14.2031(17)	10.461(4)	7.3769(9)
β, deg		112.17(1)	90.793(12)
V, Å^3	795.4(3)	1445.4(9)	692.74(16)
Z	4	4	2
space group	*Pbca*	*C*2/*c*	$P2_1/n$
fw	303.2	448.2	379.3
temp, K	293	293	293
λ, Å	0.71073	0.71073	0.71073
ρ_{calcd}, g cm^{-3}	2.06	2.06	1.82
μ, mm^{-1}	1.45	1.17	1.04
$R(F)$, $R_w(F)$*	0.023, 0.047	0.062, 0.086	0.027, 0.034

[a] $R = [\sum||F_o| - |F_c||]/[\sum|F_o|]$; $R_w = \{[\sum w||F_o| - |F_c||^2]/[\sum(w|F_o|^2)]\}^{1/2}$.

Table 6. Summary of Bond Lengths (Å)

compound	**3**	[**3**][PF_6]	**4**
S1−S2	2.0865(7)	2.0391(17)	2.0780(7)
S2−N2	1.6467(16)	1.616(4)	1.6577(16)
S1−C2	1.7402(16)	1.713(4)	1.7859(18)
N2−C1	1.2690(21)	1.305(6)	1.2708(24)
C1−C2	1.4581(22)	1.424(6)	1.4778(24)
C2−N1	1.2994(20)	1.325(5)	1.2691(25)
N1−N1′	1.381(3)	1.330(7)	
N1−C4			1.4047(23)
C4−C3			1.4025(25)
C4−C5			1.389(3)
C3−C5			1.380(3)

distribution heavily localized on the central two nitrogens. Indeed, within the series **1** (R_4 = Cl, $R_5 = C_6F_5$), $[\mathbf{2}]^+$, and $[\mathbf{3}]^+$, the drop-off in the hyperfine coupling contant to the DTA nitrogens is quite dramatic, and in $[\mathbf{3}]^+$, it is sufficiently small to be lost in the line width of the signal.

Crystal Structures. The crystal and molecular structures of **3**, [**3**][PF_6], and **4** have been determined by single-crystal X-ray diffraction. Crystal data for the three structures are compiled in Table 5 , and mean internal structural features are summarized in Table 6. ORTEP drawings of **3** and **4**, providing the atom-numbering schemes, are shown in Figure 4.

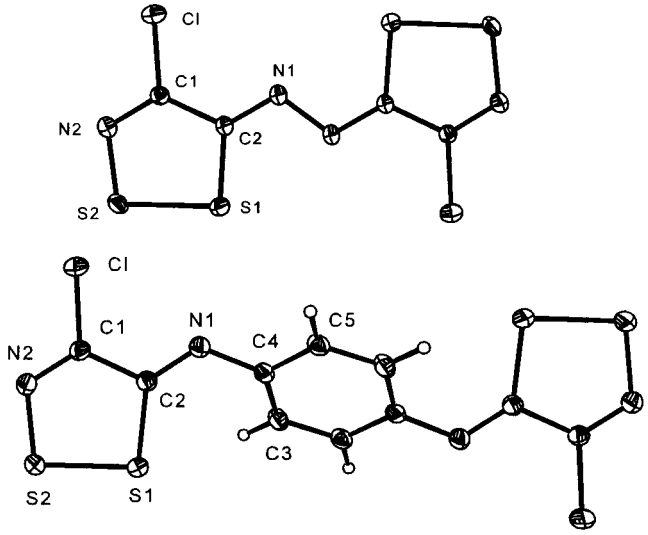

Figure 4. ORTEP drawings of **3** and **4**, showing atom numbering. The atom numbering of the cation in [**3**][PF_6] is the same as in **3**.

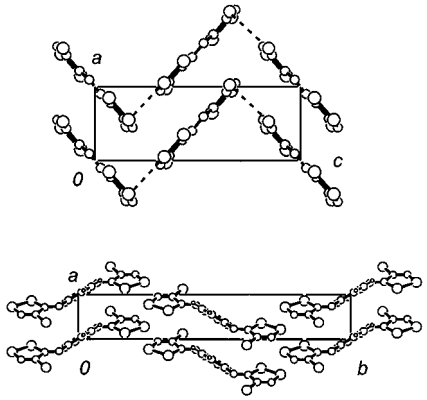

Figure 5. Views of herringbone stacks of **3** (above) and slipped π-stacks of **4** (below). The S2- - -S2′ contact in **3** (dashed line) is 3.5660(8) Å.

Molecules of **3** lie on a crystallographic center of inversion and are planar to within 0.03 Å. The internal bond lengths of the 1,2,3-DTA rings are similar to those seen in **2** and, along with the long N−N bond, are consistent with the azine resonance structure. There is also good agreement with the trends predicted by the DFT calculations (Table 2). Molecules of **4** are also crystallographically centrosymmetric but are far from planar. To avoid potential steric congestion between S1 and the C3 proton, the DTA ring (which is planar to within 0.07 Å) is rotated about the N1−C4 bond to form a dihedral angle of 137.30(7)° with the plane of the benzene ring. As a result of this torsional motion, conjugation with the benzene bridge is restricted; the C2−N1 bond in **4** is thus a more localized (shorter) double bond than the corresponding exocyclic C2−N1 bond in **3**.

Crystals of **3** consist of severely slipped stacks or herringbone arrays of molecules running parallel to the x direction (Figure 5); the interplanar spacing is 3.312(2) Å. Along these stacks, there are no intermolecular S- - -S contacts inside the van der Waals separation for sulfur (3.6 Å).[22] There is, however, one lateral interaction (S2- - -S2′ = 3.5660(8) Å), which bridges molecules in neighboring stacks. The packing of molecules in **4** consists of a more conventional slipped stack structure along x, with the registry of adjacent stacks being somewhat ruffled

(22) Bondi, A. *J. Phys. Chem.* **1964**, *68*, 441.

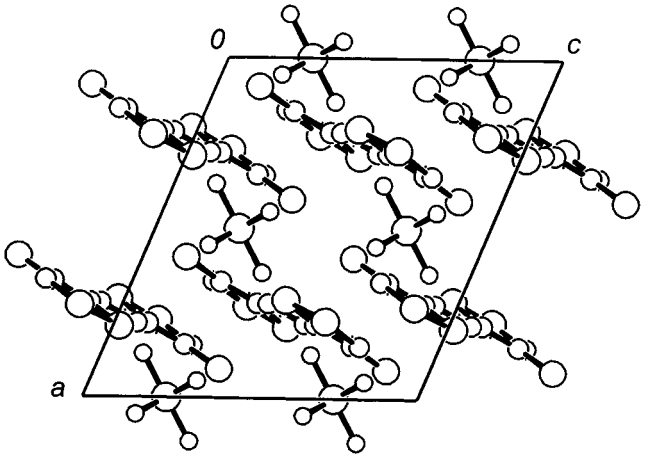

Figure 6. Packing of cations and anions in [**3**][PF_6].

by the twist in the phenylene bridge (Figure 5). Again, there are no close intermolecular S- - -S contacts along the stacks, and the only short lateral interaction is S1- - -S2′ (3.6120(8) Å).

The crystal structure of [**3**][PF_6] consists of discrete [**3**]$^+$ radical cations and PF_6^- anions (Figure 6). The cations are well-separated, with the shortest intermolecular S- - -S′ contact being 4.049(2) Å (S1-- -S2′). In this light, the low conductivity of the material is not surprising. At the molecular level, the changes in internal bond lengths as a function of oxidation state can be easily understood with reference to the DFT calculations described above and the nature of the $1b_g$ HOMO (Figure 2). Thus, the contraction in the S−S, the S−N, the S−C and, most notably, the N−N bonds, as well as the lengthening of the exocyclic C−N bonds, reflect the bonding properties of this orbital.

Summary and Conclusion

We have extended the range of 5,5′-bridged bis(dithiazoles) to include the diazine- and phenylenediamine-bridged compounds **3** and **4**. The azine derivative **3** displays well-behaved electrochemical behavior and, like **2**, can be reversibly oxidized to a radical cation and closed-shell cation. However, the highly electronegative bridging group leads to much more anodic oxidizing potentials than those seen for **2**, so that generation of air-stable CT salts by conventional chemical and electrochemical methods is not practical. Nonetheless, using acidic solvents (SO_2-(l)) and iodine trichloride as oxidant, the CT salt [**3**][ICl_2] can be generated; metathesis of the latter with $AgPF_6$ affords the corresponding hexafluorophosphate salt. As a result of steric interactions between the DTA ring and the phenylene group, the phenylenediamine bridge in **4** is twisted with respect to the two terminal DTA rings, and conjugative interactions between the two ends are minimal. No radical cation state has been observed for this compound.

Experimental Section

General Procedures and Starting Materials. 1,4-Phenylenediamine, anhydrous hydrazine, iodine trichloride, sulfur monochloride, ferrocene, and silver hexafluorophosphate were obtained commercially (Aldrich). The solvents dichloromethane (Fisher), dichloroethane (Fisher), and acetonitrile (Fisher, HPLC grade) were commercial products and were dried by distillation from P_2O_5. All reactions were carried out under 1 atm of nitrogen, save those involving liquid SO_2 as solvent. The latter were performed in vacuo using standard h-cell techniques; the sulfur dioxide gas (Matheson) was used as received. Melting points are uncorrected. Appel's salt was prepared as described in the literature,[11] with Adogen 464 (Aldrich) used as a catalyst. Elemental analyses were performed by MHW Laboratories, Phoenix, AZ. Infrared spectra were recorded (at 2 cm^{-1} resolution on Nujol mulls) on a Nicolet Avatar infrared spectrometer. Low resolution mass spectra (70 eV, EI, DEI and CI, DCI) were run on a Finnigan 4500-quadrupole mass spectrometer at the McMaster Regional Centre for Mass Spectrometry. The X-band ESR spectra of the radical cation [**3**]$^+$ (as its PF_6^- salt dissolved in SO_2(l)) were recorded on Varian E-109 and Bruker EMX spectrometers at ambient temperature (22 °C).

Synthesis of 1,4-Diimino-1*H*,4*H*-bis[4-chloro-5*H*-1,2,3-dithiazole]benzene, 4. A slurry of 1,4-phenylenediamine (519 mg, 4.80 mmol) and Appel's salt **5** (2.57 g, 12.3 mmol) in 30 mL of dichloroethane was stirred at 35 °C for 18 h under an inert atmosphere. The reaction mixture was cooled to room temperature, and the yellow precipitate of the crude dichloride salt [**4**][$Cl]_2$ was collected by filtration and washed with methylene chloride. IR (1600−400 cm^{-1}): 2670 (b), 1601 (w), 1536 (vs), 1231 (m), 1195 (m), 1014 (w), 914 (m), 865 (w), 835 (w), 816 (w), 782 (m), 700 (m), 641 (w), 618 (w), 536 (w), 515 (m), 481 (w). The crude dication [**4**][$Cl]_2$ was reduced to the neutral state **4** by washing it with ethanol. Recrystallization of the orange solid so obtained from hot toluene (15 mL per 100 mg) yielded red needlelike crystals of **4** (1.6 g, 4.22 mmol, 88%). mp 246−48 °C. IR (1600−400 cm^{-1}): 1584 (s), 1543 (w), 1483 (m), 1412 (w), 1286 (w), 1234 (m), 1220 (m), 1141 (s), 1106 (s), 1009 (w), 955 (w), 860 (s), 835 (m), 823 (m), 774 (w), 763 (s), 640 (m), 629 (s), 551 (m), 525 (s), 438 (m). UV/Vis ($CHCl_3$) λ_{max} (log ϵ) 421 (4.1) nm. MS (*m*/*z*): 378 (M^+, 21%). Anal. Calcd for $C_{10}H_4N_4S_4Cl_2$: C, 31.67; H, 1.06; N, 14.77. Found: C, 31.80; H, 0.91; N, 14.64.

Synthesis of 1,2-Bis[4-chloro-5*H*-1,2,3-dithiazole]dinitrogen, 3. A solution of anhydrous hydrazine (0.25 mL, 8.0 mmol) in 15 mL of dry dichlororethane was added dropwise to a slurry of **5** (3.125 g, 14.987 mmol) in 50 mL of dry dichloroethane held on ice, in an inert atmosphere. The red slurry was stirred at room temperature for 18 h and then refluxed for 4 h. When it was cooled to room temperature, red crystals of **3** were produced. These were collected by filtration and were recrystallized from chlorobenzene. Yield: 0.752 g (2.48 mmol, 33%). mp 249 °C. Crystals suitable for single-crystal X-ray diffraction were obtained by vacuum sublimation at 130 °C/10^{-2} Torr. IR (1600−400 cm^{-1}): 1562 (w), 1536 (s), 1505 (w), 1176 (s), 890 (s), 879 (s), 733 (w), 693 (s), 525 (m), 441 (m), 424 (m). UV/Vis ($CHCl_3$) λ_{max} (log ϵ) 505 (4.9), 472 (5.0), 455.5 (4.8) nm. MS (*m*/*z*): 302 (M^+, 47%). Anal. Calcd for $C_4N_4S_4Cl_2$: C, 15.84; H, 0.0; N, 18.48. Found: C, 16.08; H, trace; N, 18.36.

Synthesis of [3][ICl_2]. Under an inert atmosphere, **3** (0.561 g, 1.85 mmol) and iodine trichloride (0.460 g, 1.97 mmol) were loaded into an h-cell, and sulfur dioxide (10 mL) was condensed into the reaction vessel. The mixture was stirred at ambient temperature for 18 h and eventually yielded a black precipitate. This solid (crude [**3**][ICl_2]) was collected by filtration, washed with sulfur dioxide (7 × 5 mL), and dried in vacuo. Yield: 0.835 g (1.67 mmol, 90%). IR (1600−400 cm^{-1}, NaCl plates, Nujol): 1564 (w), 1530 (m), 1504 (w), 1423 (s), 1444 (s), 1205 (s), 906 (s), 828 (s), 798 (w), 711 (s).

Metathesis of [3][ICl_2] to [3][PF_6]. Silver hexafluorophosphate (0.200 g, 0.791 mmol) and [**3**][ICl_2] (0.359 g, 0.716 mmol) were loaded into an h-cell, and sulfur dioxide (10 mL) was condensed onto the solid reagents. After it was stirred for 15 min at ambient temperature, a deep blue solution formed along with a white preciptate of AgCl. The latter was filtered off, and the SO_2 was slowly removed to yield a few gold needles (uncharacterized) and black, extremely moisture-sensitive, oblong blocks of [**3**][PF_6]. IR (1600−400 cm^{-1}, NaCl plates, Nujol): 1536 (w), 1442 (s), 1426 (s), 1328 (m), 1250 (w), 1194 (s), 1145 (w), 1007 (w), 907 (s), 844 (vs), 742 (w), 710 (m). The identity of this material was confirmed by single-crystal X-ray analysis.

Cyclic Voltammetry. Cyclic voltammetry was performed on a PINE Bipotentiostat, Model AFCBP1 on solutions of **3** and **4** containing 0.1 M tetra-*n*-butylammonium hexafluorophosphate in CH_3CN (dried by distillation from P_2O_5). Potentials were scanned using scan rates of 50−250 mV s^{-1} from −2.0 to 2.5 V with respect to the quasi-reference electrode in a single compartment cell fitted with Pt electrodes and referenced to the ferrocenium/ferrocene couple at 0.38 V vs SCE.[23]

X-ray Measurements. Data were collected at 293 K on Enraf-Nonius CAD4 (**3**), Rigaku Mercury CCD ([**3**][PF_6]), and Siemens P-4 (**4**) diffractometers using $\omega-2\theta$ (**3**) and ω ([**3**][PF_6] and **4**) scans. The structures were solved by direct methods and refined by full-matrix least-squares analysis, which minimized $\Sigma w(\Delta F)^2$.

Ab Initio Calculations. All calculations on the proto version of **3** were run on Pentium II workstations using the B3LYP DFT method, as contained in the Gaussian 98W suite of programs.[24] Geometries were optimized using a 6-31G** basis set, within the constraints of C_{2h} symmetry.

Acknowledgment. We thank the Natural Sciences and Engineering Research Council of Canada and the State of Arkansas for financial support in the form of operating and equipment grants. We also acknowledge the Arkansas Science and Technology Authority for support of the X-ray facilities and the NSERCC for a post-graduate scholarship to K.E.P.

Supporting Information Available: A summary (1 page) of G98 input and output data for calculations relating to **3**, $[\mathbf{3}]^+$, and $[\mathbf{3}]^{2+}$. Crystallographic files, in CIF format, for **3**, [**3**][PF_6], and **4**. This material is available free of charge via the Internet at http://pubs.acs.org.

IC0010095

(23) Boeré, R. T.; Moock, K. H.; Parvez, M. *Z. Anorg. Allg. Chem.* **1994**, *620*, 1589.

(24) Frisch, M. J.; Trucks, G. W.; Schlegel, H. B.; Scuseria, G. E.; Robb, M. A.; Cheeseman, J. R.; Zakrzewski, V. G.; Montgomery, J. A., Jr.; Stratmann, R. E.; Burant, J. C.; Dapprich, S.; Millam, J. M.; Daniels, A. D.; Kudin, K. N.; Strain, M. C.; Farkas, O.; Tomasi, J.; Barone, V.; Cossi, M.; Cammi, R.; Mennucci, B.; Pomelli, C.; Adamo, C.; Clifford, S.; Ochterski, J.; Petersson, G. A.; Ayala, P. Y.; Cui, Q.; Morokuma, K.; Malick, D. K.; Rabuck, A. D.; Raghavachari, K.; Foresman, J. B.; Cioslowski, J.; Ortiz, J. V.; Stefanov, B. B.; Liu, G.; Liashenko, A.; Piskorz, P.; Komaromi, I.; Gomperts, R.; Martin, R. L.; Fox, D. J.; Keith, T.; Al-Laham, M. A.; Peng, C. Y.; Nanayakkara, A.; Gonzalez, C.; Challacombe, M.; Gill, P. M. W.; Johnson, B. G.; Chen, W.; Wong, M. W.; Andres, J. L.; Head-Gordon, M.; Replogle, E. S.; Pople, J. A. *Gaussian 98*; Gaussian, Inc.: Pittsburgh, PA, 1998.